Accepted Manuscript

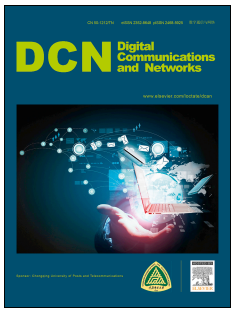

Recent advancements in surface plasmon polaritons- plasmonics in subwavelength structures at microwave and terahertz regime

Rana Sadaf Anwar, HuanSheng Ning, LingFeng Mao

PII: S2352-8648(17)30199-2

DOI: 10.1016/j.dcan.2017.08.004

Reference: DCAN 98

To appear in: *Digital Communications and Networks*

Received Date: 20 June 2017

Revised Date: 2352-8648 2352-8648

Accepted Date: 9 August 2017

Please cite this article as: R.S. Anwar, H. Ning, L. Mao, Recent advancements in surface plasmon polaritons- plasmonics in subwavelength structures at microwave and terahertz regime, *Digital Communications and Networks* (2017), doi: 10.1016/j.dcan.2017.08.004.

Recent advancements in Surface Plasmon Polaritons-Plasmonics in Subwavelength Structures at Microwave and Terahertz regime

Rana Sadaf Anwar*, HuanSheng Ning, LingFeng Mao

School of computer and communication Engineering, University of Science and Technology, Beijing, China, 100083

Abstract

A review of recent investigational studies has been presented in this paper of exciting the surface plasmon polaritons (SPPs) in microwave (MW) and terahertz (THz) regime by using subwavelength corrugated patterns on conducting or metal surfaces. This article also outlines the significance of SPPs microstrip (MS) structures at microwave and terahertz frequencies, compared to the conventional MS transmission lines (TL) to tackle the key challenges of high gain, broader bandwidth, compactness, TL losses and signal integrity in high-end electronics devices. Having subwavelength properties, surface plasmon polaritons are getting fame for their improved performance and ability of miniaturization in high-speed dense circuits. They possess comparably minuscule wavelength than the incident light (photons). Consequently, they can demonstrate stronger spatial confinement and higher local field intensity at optical frequencies. Besides of engineering spoof SPPs waveguides by engraving grooves and slits on metal surfaces to operate at low frequencies (microwave and terahertz), semiconductors with smaller permittivity values and thus lower free charge carrier concentration, have been proved as a potential candidate in plasmonic devices. If necessary, further tuning of SPP structures based on a semiconductor is aided by controlling the charge carrier concentration through doping, or by external stimuli such as optical illumination or thermal excitation of charge carriers from valence to conduction bands. This article conclusively covers perspectives of manipulating SPPs in MW and THz range that have so far been elucidated and emphasizes how these could steer the next-generation plasmonic devices.

Keywords: Surface plasmons; Subwavelength; Metamaterials; Plasmonics; Terahertz; Microwave

1. Introduction

Plasmonics is an emerging area of science and technology in which propagation of light can be controlled by the use of subwavelength structures. Focused applications of plasmonics are numerous such as surface-enhanced Raman scattering [1], surface plasmon resonance sensors [2], surface plasmon spectroscopy systems [3-5]. Diverse of fields have hugely been benefited, ranging from chemistry, biology, physics, and material science [6-8].

The basic ability from which plasmonics is benefited, is confining the EM fields into smaller scales, in contrast to other conventional focusing techniques, like dielectric lenses[9, 10]. Many applications are supported by this inherent characteristics, for instance, improved collection of EM energy (such as, in photovoltaic applications) [11-14], better spatial resolution imaging [15, 16], and in nonlinear devices, e.g., lasers [17-19]. Also, the phenomenon is fully applied for sensing purposes in biochemistry [20-22], control switches, signal amplifiers and modulators based on SPPs [23-27].

Bethe [28] in 1942, predicted that transmission intensity of EM waves through circular subwavelength opening designed in an optically thick metal layer is proportional to $(d/\lambda)^4$, where d is the diameter of circular openings and λ is the wavelength of the light. R. H. Ritchie [29] in 1957 discovered that fast moving electrons lost their energy when passed through a thin metal film. He predicted that it may be due to the self-sustained oscillations that existed at the metal surfaces. Later, Powell and Swan proved the same mechanism through experiments [30]. Raether [31] also spotted the unique behavior of metals of having easily accessible collective excitations of electrons. Years after these predictions, in 1998, Ebbesen et al. [32], made intensive research and investigated extraordinary optical transmission across periodic arrays of holes milled in optically thick metal film. Unusual transmission of light was discovered, which was orders of magnitude higher than

* Corresponding author. Tel.: +86-13011210900
E-mail address: engr_rs@126.com

those theoretically anticipated by Bethe in classical aperture theory. Following this invention, a lot of experiments and theoretical research has been carried out, to clarify the hidden phenomenon and resulted in significant advancements in plasmonic applications [32-38].

Finally, it was postulated that the interaction of light waves with free electrons on the metal-dielectric interface, create surface plasmons. Under certain conditions, due to the positive permittivity of the dielectric material and negative permittivity behavior of metal at optical frequencies, the incident light combines with the surface plasmons, thereby creating self-sustaining and propagating EM waves, known as surface plasmon polaritons [9]. Once they are excited, the SPPs travel in a parallel direction along the metal-dielectric interface. SPPs have much smaller wavelength compared to the incident light. Their primitive existence is temporary and they decay exponentially along the direction perpendicular to the metal-dielectric interface. It has been proved that SPPs provoke on the metal-dielectric interface and incident energy can easily cross through the edges of the periodic corrugations in metal film around where it is highly accumulated [32, 39-43].

As thoroughly explored, SPPs are related to a wider category of electromagnetic solutions generally named as Zenneck wave or sommerfield waves whose confinement is weak on the surface [44-46]. However, SPPs are propagating waves that highly localize the EM field on the conducting surface[31]. Regardless of their excellent plasmonic properties of stronger field confinement and enhancement on metal surfaces in optical regime [10], SPPs cannot be excited naturally at low frequencies in THz/MW bands where a metal behaves as perfect electric conductor (PEC) [47]. To overcome this predicament and provoke highly confined SPPs at lower frequency regime, spoof surface plasmon polaritons (SSPPs) have been proposed with the concept of employing metamaterials [48, 49]. Surface decorations are supplemented in the form of grooves, holes, slits and blocks on the conducting surfaces at deep subwavelength scale to support SSPPs at MW and THz scale [47, 49-52]. These plasmonic metamaterials include a one-dimensional array of grooves at subwavelength scales [50, 53], two-dimensional arrays of pits or hills [48, 49, 54], or three-dimensional periodic arrays of circular grooves in perfect conducting wires [55]. They mimic the exotic properties of natural SPPs, and their dispersion characteristics and spatial confinement can be engineered at will by adjusting the geometrical parameters [12, 50, 54-60].Hence, they have paved a path to realize SPPs at lower frequency, exhibiting similar properties like natural SPPs in the optical regime.

However, all the above mentioned surface decorations are not convenient to fabricate and integrate, due to their dimensional structure vertically above or below the conducting surface. Specifically, due to the complex and three-dimensional design structures of most recently developed plasmonic metamaterials (having larger volumes), they cannot lie in the class of transmission lines. Therefore, a new type of compact planar spoof SPP structures have been proposed, which are etched on the standard printed circuit board technology [61-69]. These compact SSPPs are the most promising candidate in microwave circuits, consumer electronics and systems owing to their ultra-thinness, flexibility, and reduced fabrication cost.

With the ability of exciting EM waves on a subwavelength scale, SPPs have been widely adapted in the THz application. Although, it was expected at first that high conductivities of metals could be an impediment in the demonstration of SPPs in THz range. In contrast, SPPs have successfully been excited on metal-dielectric interfaces using prism coupling, evanescent field coupling [70-73], and through two-dimensional aperture arrays in metals [74-83]. A number of practical applications have been cultivated by the proficient use of SPPs at THz frequencies, such as in the field of chemical as well as biological spectroscopy, high-frequency communication, accurate sensors, optical antennas, modern imaging technology, photo-detectors, electron energy loss spectroscopy, cathodo-luminescence, security and surveillance, non-destructive spectroscopy, biosensor and a lot of many others [84-94]. Keeping in view the gigantically used concept of plasmonics, the research area has been proved full of surprises in last decade and is likely to uncover numerous alluring prospective applications.

The innovation brought by area of plasmonics has enabled the upcoming SPPs based structures and devices to conquer many technological obstacles. The purpose of this paper is to present an overview of the properties of SPPs and examine how they work on subwavelength scale and THz range. We will present the important

results investigated by a few researchers, such as dispersion diagrams and scattering parameters (transmission and reflection coefficients). The paper is organized as follows: In section 1, concept of surface plasmon polaritons is developed along with the motivation behind studies of SPPs in MW and THz regime. Section II illustrates the theoretical background of SPPs with dispersion diagram. Role of plasma frequency and permittivity in realization of SPPs is also discussed. A brief overview of SPPs excitation on doped semiconductors is also mentioned. Section III describes the general model of surface plasmonic waveguide. Section IV covers a brief overview and analysis of some investigational research presented in this field, aimed to explicate the effect of varying certain design parameters on SPPs excitation. Section V provides brief concluding comments and outlook.

2.1 Motivation of SPPs Studies

High gain, broader bandwidth, compactness, suppression of transmission line losses in microstrip lines, and signal integrity are the key challenges in high-end electronic devices, integrated circuits, and systems[61, 95]. Currently, these issues are inevitable in communication devices and high-speed applications. Mutual coupling is another substantial problem in dense circuits with a huge number of parallel transmission lines [96].

All passive and active devices are based on transmission lines, being the key element of transmitting data. Microstrip is the commonly used transmission line in microwave and millimeter wave frequencies and is easy to fabricate. Therefore, it has been extensively used in compact, light weight circuits, and antennas. However, it has drawbacks of narrow bandwidth, susceptibility to crosstalk, low gain, and poses comparatively large TL losses. The efficient designs of MS TLs are desirable to flourish and satisfy the needs of high-speed communication devices in the modern era of electronics.

Transmission of EM pulses has been demonstrated in metal structures with periodic openings in electromagnetic spectrum, having a broad range of optical, infrared and microwave frequencies [32-36, 43, 55, 77, 97-99]. Having excellent transmission characteristics, SPPs structure may be regarded as the most auspicious nominee in THz frequencies, MW circuits, commercial electronics applications, and systems. Also, the construction of spoof surface plasmon polaritons (SSPPs) and afterward, ultrathin conformal surface plasmons (CSPs) structures [66] provide the basis of flexible plasmonic structure designs and so direct a way to conveniently transmit EM waves in MW and THz regime [51, 95, 96]. However, SSPPs devices are difficult to function independently due to the problem in feeding and extracting signals efficiently from plasmonic waveguide [51, 95, 100]. Therefore, the major obstruction in realizing SSPPs at MW frequencies lies in bridging the transition structure for conversion from conventional microwave circuit (e.g. microstrip, coplanar waveguides or plotline) to SSPP devices, so as to maximize the efficiency and bandwidth. Some techniques have been presented by drilling symmetric or unsymmetrical periodic and gradient grooves [63, 65, 67, 101-105] and intensive research is proceeding in the area of smoothing out this transition.

Miniaturization in high-speed circuits and systems based on SPP structures can be achieved by the removal of unwanted filtering circuit. Zhang et al. demonstrated in [61] that by varying the grooves depth, the dispersion curves exhibit a corresponding cutoff frequency. When the operating frequency becomes greater than this cut-off frequency, no more propagation of SPP waves is possible through the plasmonic waveguide which is depicted by a sudden decline in the transmission spectrum. Therefore, this innate phenomenon in SPPs facilitate the filtering purpose and is used in achieving miniaturization of plasmonic devices [63, 65].

TL losses may prominently deteriorate the performance of the whole system if not properly addressed. Controlling these losses is a difficult task by adjusting the parameters of the structure in microstrip TLs. To cope with this problem, most of the research is focused on using low loss materials [106] or by adding low dielectric material layers; consequently , addition of design complexity and cost. SPPs provide a solution to the problem of TL losses with its attractive feature of alterable wave number [48, 95]. Zhang et al. [61] proved through numerical simulations and experiment that transmission loss in a well-designed SPPs TL is quite smaller than same sized conventional microstrip TL over a wide band of microwave frequencies. In

conventional MS coupled lines, coupling coefficient increases with the increase of propagation constant. In contrast to this fact, it has been demonstrated that SPPs result in tighter field confinement when the propagation constant is increased and hence, the field overlapping factor is also reduced. This feature makes SPPs low loss waveguides, for which the transmission power is approximately independent of the coupling length [61].

High speed circuits extensively use differential microstrip transmission lines to reduce the crosstalk, compared to single ended microstrip lines. Nevertheless, in advanced dense electronic circuits, the neighboring circuitry could cause common mode effects even in these less noisy differential signal pairs and thus the crosstalk noise cannot be ignored. It has been claimed by Wu et al. that the EM field can be tightly confined inside the corrugations on differential MS lines as compared to conventional MS and therefore, crosstalk between the differential pair can be effectively reduced [96]. It also helps to suppress the conversion of the differential signal to the common mode signal. Propagation length of these lines is also high enough and experiment in time domain has proved that they are well suited in high-speed circuitry. Symmetric subwavelength corrugations are introduced on two MS differential lines, therefore improving the EM penetrations into the metallic surface and stronger field confinement can reduce the crosstalk and suppress the conversion effect very efficiently. Trapping the EM waves with the help of plasmonic structures results in confining and controlling the velocities of light and EM waves and hence, this phenomenon is used for applications in adding optical delays, optical modulation, optical buffers, and switching operation at MW and optical frequencies [107]. Plasmonic structures having an ultra-thin metallic film with non-uniform gradient corrugations, have been reported to slow down the SPP waves gradually in THz and MW regime and are reflected at the predesigned locations when the frequency is changed [108].

2. Theory of Surface Plasmon Polaritons - Dispersion relation

Initially, SPPs studies were targeted in visible and infrared light region. Extraordinary optical transmission through metallic subwavelength grating arrays opened a new era of realizing SPPs excitation at low frequencies (MW and THz). To understand intrinsic aspects of SPPs, dispersion diagram can greatly help, which relates the angular frequency with momentum (also called in-plane wavevector) in SPP modes.

The Dielectric constant of metals is given by Drude model and is related to plasma frequency as

$$\varepsilon_M(\omega) = 1 - \frac{\omega_P^2}{\omega^2 - i\Gamma\omega} \qquad (1)$$

Where

$$\omega_P = \sqrt{ne^2 / m\varepsilon_0} \qquad (2)$$

Here, ω_P is the bulk plasma frequency, ω is the angular frequency of incident EM wave, Γ is the scattering rate of electrons motion, ϵ_0 is the permittivity of free space, n is the free carrier density, while e and m are the charge and the mass of an electron respectively. Metals have a higher density of free electrons, so they have higher plasma frequency. This property makes the metal as a material of choice for plasmonic applications. In most of the metals, plasma frequency spans from infrared to ultraviolet range. When the frequency of incident EM is less than the plasma frequency, the dielectric function becomes imaginary. Therefore, propagation of light through metal is greatly attenuated. On the other hand, Ritchie in [29] and further investigational studies confirm that SPPs propagate in a broader range of frequencies from $\omega = 0$ to $\omega = \omega_P / \sqrt{2}$, along the direction parallel to the metal-dielectric interface. Fig. 1 shows a pictorial view of SPPs propagating along the direction parallel to the metal-dielectric interface, also displays exponential decaying z-component of the electric field. Wavenumber (K) defines the decay of the EM field with the increase of distance from the

surface [109] and it determines the dispersion of the EM wave. Dispersion relation of light in a metal is obtained by substituting dielectric constant relation in Maxwell's equation and is given as

$$\omega^2 = (Kc)^2 + \omega_P \tag{3}$$

ω is the angular frequency of incident EM field and c is the speed of light. The in-plane wavevector K_x or momentum of SPPs is the wavevector in the plane of the surface along which it propagates and is a function of angular frequency [31]

$$K_x = K_0 \sqrt{\frac{\varepsilon_I \varepsilon_M}{(\varepsilon_I + \varepsilon_M)}} \tag{4}$$

ε_M and ε_I are the frequency dependent complex dielectric functions (relative permittivity) of metal and adjacent dielectric medium respectively. $K_0 = \omega/c$ is the free-space wavevector. Also $\varepsilon_M = \varepsilon_{MR} + i\varepsilon_{MI}$, Where ε_{MR} and ε_{MI} are defined as real and imaginary parts of the relative permittivity of metal. ε_{MR} describes the strength of polarization induced by an external electric field while ε_{MI} explains the absorption and scattering losses encountered when materials interact with EM waves. The relative permittivity of dielectric material ε_I is inadequately dispersive; therefore, relative permittivity of metal plays a major role in the excitation of SPPs, which ultimately controls the behavior of extraordinary transmission. As a matter of fact, charges on the surface of a metal are involved in provoking SPPs. To sustain these charges, component of electric field normal to metal-dielectric interface (E_z from fig.1) must change its sign throughout the interface. The component of displacement field in normal direction of surface (D_z) needs to be constant, to satisfy the equation $D_z = \varepsilon E_Z$. Consequently, to support the SPP excitation, the sign of ε_M and ε_I must be opposite. It is known that the value of ε_I is real and positive, so this puts a restriction on the relative permittivity of the metal ε_M , to be real and negative. At optical frequencies, many metals have a negative dielectric permittivity, largely consisting of negative real part while the positive imaginary part is tiny.

Because, wavevector of free space photon (in the dielectric medium, it is $\sqrt{\varepsilon_I}K_0$) adjoining the metal, is less than the wavevector of SPPs (K_{SP}) at the same frequency. Therefore, only if this momentum is matched to momentum of SPPs (K_{SP}), at that instance the SPPs may be excited by the free propagating EM waves. Momentum matching has been achieved through different techniques, which employ scattering of EM waves by structure design such as using high index prism, evanescent field coupling and grating coupling [71, 72, 82]. However, SPPs transmission by using periodic aperture arrays has been investigated excessively.

At surface plasmon frequency, $K_x \to \infty$ and

$$\mathrm{Re}[\varepsilon_M] = -\varepsilon_I \, (\varepsilon_I > 0) \tag{5}$$

$$\omega = \frac{\omega_P}{\sqrt{1+\varepsilon_M}} \tag{6}$$

Dispersion curve in Fig. 2 gives a graphical illustration of frequency versus wavevector relation. Here, there are two cases to be identified (see fig.2):

When $\omega < \omega_P$, then the permittivity of metal ε_M is real and negative. Dispersion curve of SPPs lies to the right and closer to the dispersion curve of the light line. It means the surface plasmon polaritons have a higher wavevector than the light waves of the same frequency, propagating along the surface [31]. Wavevector of EM wave in medium is imaginary, and EM wave decays exponentially and in the direction perpendicular to the surface. As frequency increases, the SPP mode deviates away from the

light line until it reaches an asymptotic resonant frequency ω_{SP}. At this frequency, ε_M is equal to ε_I but with an opposite sign. When $\omega > \omega_P$, ε_M is real and positive. Wavenumber is real, and therefore no wave decay takes place, and wave propagates as it travels in the ordinary positive dielectric medium [109, 110] as given by the theory of Drude.

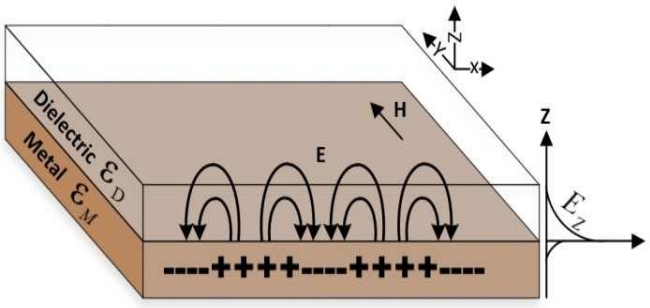

Fig. 1. Surface plasmon polaritons propagation

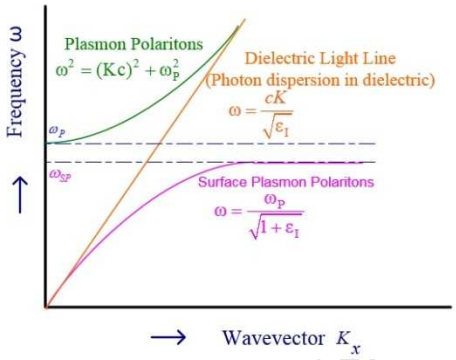

Fig. 2. Dispersion curve of SPPs on metal-dielectric interface

2.1 SPPs on doped semiconductors

Because plasma frequency is proportional to the free carrier density ($\omega_p \propto n$) in Eq. (2) therefore, we may control ω_p by varying charge carrier density. Periodic structured metals (corrugated design) may provide this facility and support the excitation of SPPs [111]. On the other hand, by changing the doping level in the semiconductors may stimulate the surface waves [112, 113], specifically highly doped semiconductors excite the SPPs near the THz spectrum [75, 77, 114]. Therefore, similar to SPPs excitation in metals in optical regime, highly doped semiconductors can provoke SPPs at THz frequencies. Zhang et al. [115] has pointed out that when the doping level of n-type doped silicon is increased above $1 \times 10^{17}\text{cm}^{-3}$, the real part of permittivity shows off a negative behavior at 1THz. Fig. 3. shows real and imaginary parts of permittivity of n-type silicon at 1THz as a function of carrier density. Azad et al. [75] fabricated elliptical hole arrays on a 50μm thick highly doped n-type silicon structure($3 \times 10^{19}\text{cm}^{-3}$)and successfully demonstrated the resonance frequency of SPPs at 1.6GHz with complex conductivity of 557+i100S/cm. Fig. 4 (i) shows the sample investigated and Fig .4 (ii) frequency dependent real and imaginary permittivitties of doped n-type silicon. It indicates that high doping concentration is needed to excite SPP in THz range and enhanced transmission is made possible through subwavelength corrugated arrays on these highly doped semiconducting materials [75, 77].

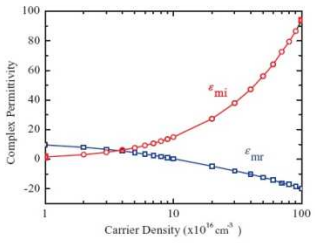

Fig.3.

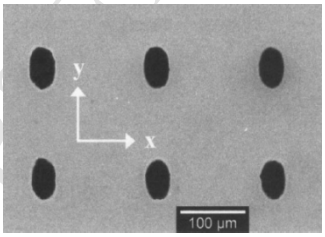

Fig4.(i)

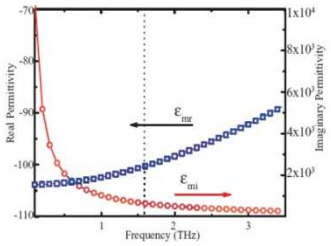

Fig.4.(ii)

Fig. 3. Real and imaginary parts of permittivity of n-type silicon at 1THz as a function of carrier density. [115] Fig. 4. [75] (i) Sample investigated with elliptical hole arrays on a thick highly doped n-type silicon structure (ii) The frequency dependent real and imaginary permittivitties of doped n-type silicon.

Additionally, Rivas et al. [116] presented the temperature dependence of the extraordinary transmission of THz waves through arrays of subwavelength gratings on a heavily doped n-type silicon with $1 \times 10^{18}\text{cm}^{-3}$carrier concentration. Likewise, optical control of SPPs transmission in THz range has been explained by Janke et al. [117] and Zhang et al. [118], which is verified through an array of holes on doped semiconductors.

3. SPPs Transmission Line Generic Structure

Microstrip transmission lines (MS TL) have frequently been used in many communication applications, as these can be simply realized by the use of printed circuit technology that is why, they are low in cost.

3.1 Subwavelength corrugated plasmonic structure design and related parameters

The subwavelength periodic corrugated array structures have been demonstrated at wide frequency spectrum from microwave to the optical regime for the excitation of surface modes. The resonant frequency of EM wave transmitted is determined mainly by the period of an array of holes, grooves etc. Structure parameters such as, gratings shape, aspect ratio of corrugations and arrays type, play a vital role in determining the strength of resonance and corresponding dispersion curves. Garcia et al. [50] illustrated that plasma frequency of surface modes depends directly on the geometry of the grooves/ holes in a semi-infinite perfect conductor with perforations in the form of one-dimensional grooves arrays or two-dimensional holes arrays. It means, for such a structure, EM response is dictated by these surface modes and can be modified at will at any required frequency in THz range (from zero to threshold frequency) by tuning the geometrical parameters of surface corrugations. In Fig. 5, one-dimensional array of grooves are corrugated on perfect conducting surface with a width W and grooves depth H. Array of grooves are separated by a specific distance also called period P [50].

For a perforated conducting surface to behave as an effective medium, the width of grooves is considered much smaller than the wavelength of light $W \ll \lambda_0$. Furthermore, to simplify, it is assumed that $P \ll \lambda_0$. For real surface mode having an evanescent incident plane wave, parallel wavevector must be greater than the wavevector of a photon in free space [50, 119].

$$K_x > K_0 \tag{7}$$

Here K_x is the parallel momentum of the incident plane wave (parallel wavevector) and $K_0$is the free-space wavevector. Based on certain assumptions and simplifications, dispersion relation of surface modes is given as [50]:

$$\frac{\sqrt{K_x^2 - K_0^2}}{K_0} = \left(\frac{W}{P}\right)\tan(K_0 H) \tag{8}$$

With higher K_x, ω tends to reach closer to $\pi c/2H$ in this case while in SPP modes, angular frequency gets to $\frac{\omega_p}{\sqrt{2}}$.

Excitation of SPPs in MS structure is possible by engineering them with subwavelength corrugations. Dispersion properties of SPPs are dependent on the dimensions as well as the shape of the gratings, and can be adjusted at will for required gain, resonant frequency and return loss. Presented by Gao et al. [63], Fig. 6 shows a spoof SPP filter with double MS lines having periodic corrugations etched on the metal plate. To improve the confinement of the Spoof SPP waves in the structure gaps and therefore, suppress the radiation loss in the y-direction (as in Fig. 6.), both metallic strips are placed in opposite direction to each other with

some separation distance S [63]. It is demonstrated that electric fields are concentrated much higher in double grating structure as compared to the single grating as seen from Fig.7.(a) and 7.(b). The electric field decreases in single grating structure along the observed line in x-direction while it has high magnitude in double grating as seen from Fig.7.c. Based on the such plasmonic waveguide, a high performance ultra-wideband plasmonic filter was designed in [63]. They proved that two parameters, groove depth (H) and gap (S) could effectively control the upper cutoff frequency of pass-band. However, both factors have a little influence on the lower cutoff frequency. Hence, the operational bandwidth can conveniently be controlled by only adjusting the groove depth or the separation gap.

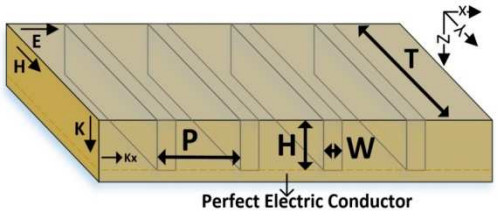

Fig. 5. One-dimensional array of grooves [50]

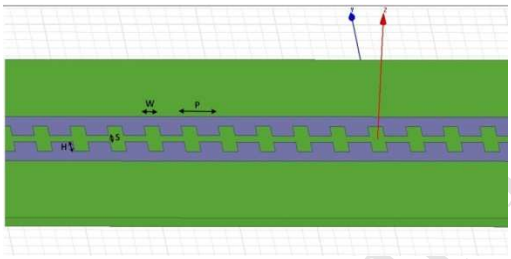

Fig.6. Dual line spoof SPPs metal strips with gratings [63]

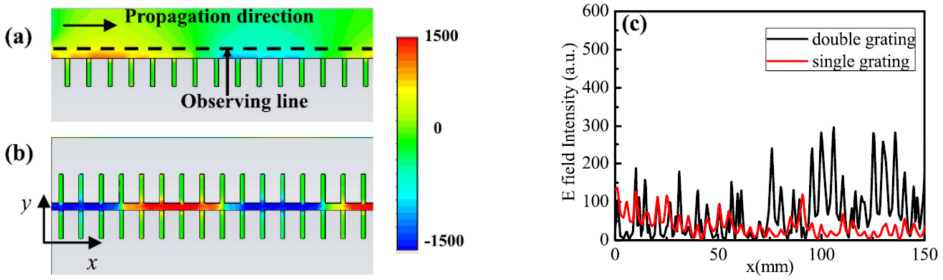

Fig. 7. The electric field distributions at 4 GHz. (a) & (b) Ey-field distributions in the xy-plane in single and double gratings, respectively. (c) Ex-field distributions along the observing line [63]

A significant advancement in microwave and terahertz range is the invention of ultrathin conformal SPP (CSP) structures, confirming flexibility and broadband features [66]. Because of these advantageous attributes which are usually required in smart and dense devices, they can be wrapped around curved structures to facilitate the conformal surface plasmons. The classic three layers flexible copper clad laminate (FCCL) plasmonic structure is designed in by Shen et al. using standard PCB fabrication process in [66] consisting of a single layer of polyimide and an electrolytic copper clad sheet connected with the epoxy adhesive shown in Fig.8 . Overall FCCL thickness of 43.5mm is kept comparably smaller than the wavelength to operate in microwave frequency range.

Shen et al. [62] proposed a free-standing comb shaped planar plasmonic metamaterial, having metal film thickness nearly equal to zero to investigate the confinement of SPP modes. A periodic array of grooves is corrugated on a perfectly conducting metal strip with thickness ‘t’, depth ‘d’, width ‘a’, period ‘p’, and height h as shown in Fig. 9.(i). Dispersion curves are calculated by using the full-wave finite-element method of the TM-polarized waves propagating in the x direction along the grooved metal strip. It has been proved that the EM waves are weakly bounded on the surface of the corrugated metal plate when the wavenumber is small enough; rather they are more tightly bound when the wavenumber is increased. They examined that the dispersion curve deviates away from the light line significantly when the thickness of the corrugated metal film is decreased and results in lower cutoff frequency. This shows an inverse trend to the dispersion relation

with lateral widths variation of Domino plasmons, standing on a metal ground layer [60]. It demonstrates the confinement of surface waves stronger on thinner metal film. Interestingly, below a metal thickness of 1µm, dispersion characteristics do not change anymore, implying that plasmonic mode is not sensitive to thickness variation. This suggests that SPPs are highly confinable on metal film with nearly zero thickness. Fig.9. (ii) shows dispersion graph of spoof SPP in THz regime [62] showing the trends by varying the thickness of metal strip from maximum to minimum, in which light line is also displayed.

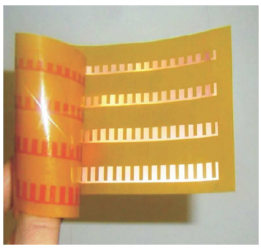

Fig.8.

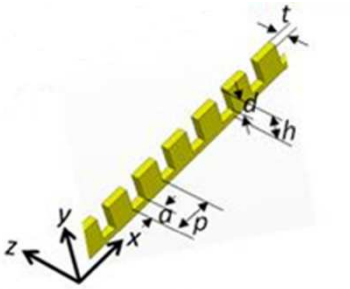

Fig.9. (i)

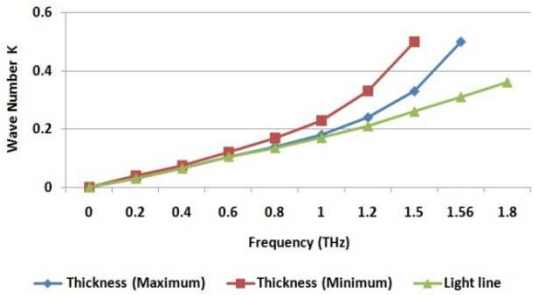

Fig.9. (ii)

Fig. 8. Fabricated sample of an ultrathin, flexible plasmonic metamaterials using FCCL. [66] Fig. 9. (i) The corrugated metal strip (ii) Dispersion graph of spoof SPP in THz regime showing the trends by varying the thickness of metal strip from maximum to minimum, Green line indicates the light line [62].

Zhang et al. [61] confirmed that microstrip lines and plasmonic waveguides demonstrate approximately similar transmission behavior below the cutoff frequency. Simulations and experiments were performed on two closely packed plasmonic waveguides (corrugated and printed anti-symmetrically on top and bottom sides of a dielectric substrate) having separation distance S shown in Fig.10. (i) . In addition, for comparison, two closely packed microstrip lines were fabricated. SPP waveguides and microstrip lines were constructed with same geometric dimensions. Fig.10. (ii) shows the fabricated samples. Two plasmonic waveguides have exhibited lower mutual coupling when the separation interval increases as compared to microstrip lines. Proposed Spoof SPPs structure can be a striking choice in dense, high-speed circuit designs requiring reduced coupling.

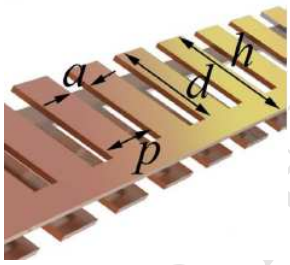

(i)

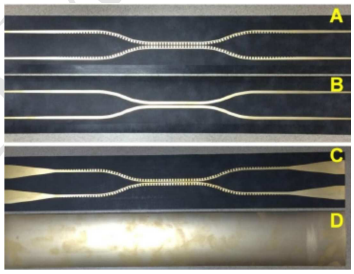

(ii)

Fig. 10. (i) Detailed structure of two closely packed spoof SPP waveguides (ii) The fabricated samples of the two closely-packed transmission lines in which (A and C) are top & bottom views of two closely-packed SPP waveguides and (B and D) are top & bottom views of two closely-packed microstrip lines [61]

Figs.11 (A-D) illustrate the trend graphs of simulation results for transmission and coupling coefficients versus frequency (GHz), performed on the structures of two closely packed SPP waveguides and microstrip lines with varying separation interval (low=0.6mm to high=2mm). Gray Shaded area exhibits the estimated data in between, with a variation of separation distance from low to high. The transmission spectra of

plasmonic waveguides shows stability in pass-band, as the separation interval increases (0.8mm to 2mm), which indicates low crosstalk is maintained. While in microstrip case, with a decrease of separation interval S, transmission curves demonstrate significantly poor performance and the crosstalk is prominently increased.

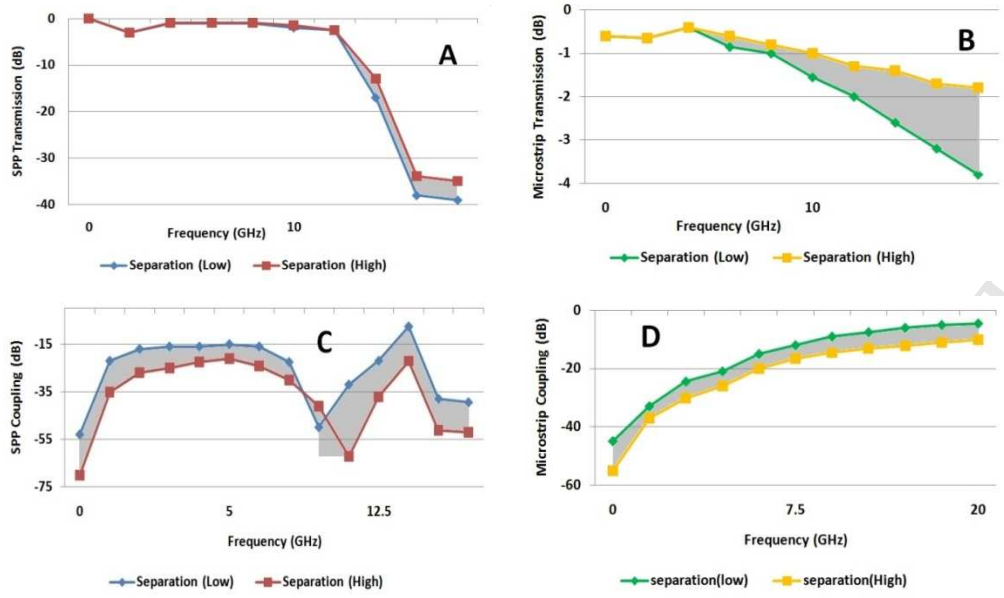

Fig. 11.Transmission and coupling coefficient versus frequency trend graph [61]. (A) SPPs Transmission (B) Microstrip Transmission (C) SPP coupling (D) Microstrip coupling

4. Earlier Research Review and Analysis

Wu et al. (2014) presented two types of novel differential microstrip lines (DLs) based on spoof SPP having symmetric, periodic corrugations of subwavelength scale on their edges [96]. The period of these corrugations is kept much smaller than operating wavelength to confirm strong confinement of EM field. Standard PCB thickness is used in fabricated microstrip (MS) lines (0.0175mm), and RO4003 is employed as substrate (Єr=3.37). Characteristics impedance of 50 Ohm for single ended lines and 100 Ohm for DLs is achieved by adjusting the width of transmission lines. Results are compared among unilateral periodic corrugated (UPC) DLs and symmetric (bilateral) periodic corrugated (SPC) DLs. Practical coupling circuits based on these DLs is also analyzed as shown in Fig.12. (a & b) It has been pointed that EM field can be more tightly confined inside the corrugations of these differential microstrip lines as compared to conventional differential microstrip lines clearly seen in Fig.12. (c) . It is demonstrated that the operating bandwidth is clearly related to the period as well as the shape of corrugations. These corrugated DLs demonstrate lesser transmission loss at low frequency in a wide band, thus proving them appropriate for long distant communication. Furthermore, crosstalk between differential lines with periodic corrugations (both UPC & SPC) and nearby microstrip line is decreased effectively. However, the period of corrugations plays a major role in suppressing the crosstalk. Differential corrugated microstrip lines with smaller period function better than the conventional differential pair in reducing crosstalk. However, UPC differential lines show better performance compared to SPC differential lines. Additionally, conversion from a differential signal to common mode signal is efficiently reduced. Time domain signal transmission through these corrugated DLs (Fig.13. (a-c)) demonstrates that they perform best in high-speed circuits, proving them a potential candidate to cope signal integrity problems in dense microwave applications.

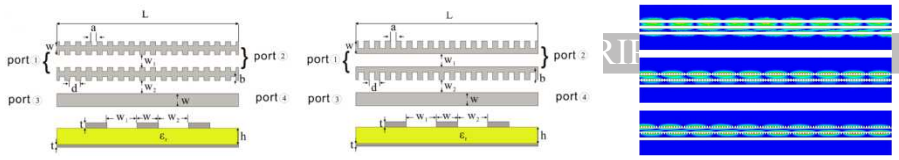

Fig.12. (a and b) Couplers composed of SPC differential MS lines/single-ended MS line and UPC differential MS lines/single-ended MS line respectively. (c) Electric field distributions simulated under the Traditional MS, SPC and UPC differential MS lines for period d = 1 mm at 8GHz.[96]

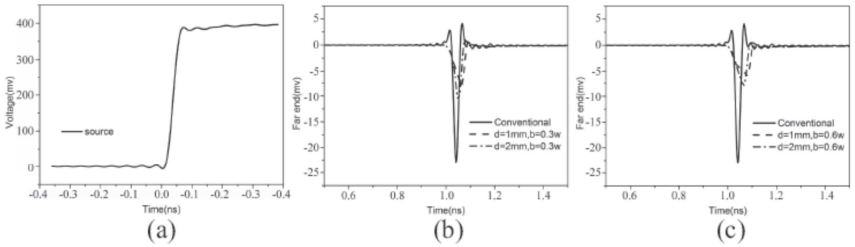

Fig. 13. Measured Results [96] (a) Input time domain signal at Port1 (b) Far-end crosstalk between SPC differential lines and MS line (c) Far-end crosstalk between UPC differential lines and MS line.

Liu et al. (2015) reported a spoof SPPs based ultrathin wideband low pass plasmonic filter with two parallel metallic strips in mirror symmetry and having symmetrical grooves etched in on opposite side of a substrate as shown in Fig.14. [100]. The filter is divided into four design sections to achieve better performance and broadband conversion between the traditional microstrip line and the symmetrical spoof SPPs. With increasing height of the grooves, dispersion curves further deviate from the light line, validating the slow propagation of SSPPs and stronger field confinement on the surfaces of the two corrugated parallel strips. For 0-10 GHz frequency band, low pass filtering operation is affirmed since the reflection coefficient remains below -10dB while the transmission coefficient sits higher over -0.6dB.

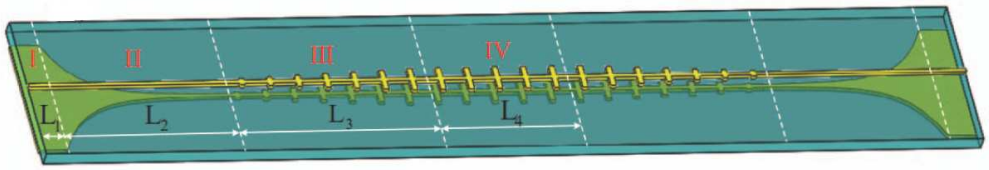

Fig.14. The geometry configuration of a plasmonic waveguide [100]

Zhang et al. [61] in 2015 proposed the time domain spoof SPPs as signals carrier, to overcome the three core challenges in the design of advanced ICs and communication systems including signal integrity, noise suppression and device shrinkage [61]. As previously discussed in section.3 and shown in Fig. 10. Ultrathin, corrugated, dual metallic strips are designed on opposite sides of the double-sided structure with mirror symmetry having Roggers RT5880 as dielectric substrate (Ɛr=2.2, tanδ=0.0009). When these waveguides are rigidly packed with deep subwavelength separation distance, they support spoof SPPs from extremely low frequency to the cutoff frequency, which can be transferred to time domain SPPs. They demonstrate improved propagation characteristics and far lesser mutual coupling than exhibited by the conventional microstrip lines. Prominent noise reduction and compactness is achieved, thereby improving the signal integrity in dense electronics circuits. Fig.15. (A) depicts that with the increase of corrugations depth, dispersion curves show

gradual deviation from MS line and further away from the light line until the cutoff frequency is reached, thus proving better slow wave performance. Transmission coefficients are recorded to be approximately 0dB (unity) for 0 to 12GHz range from Fig.15. (B). Ignorable noise is seen in transmitted time domain SPPs signal in Fig.15. (C), in response to a Gaussian input pulse with wideband of 0-12GHz. The coupling coefficient is related to the propagation constant, therefore, the coupling coefficient augments gradually in conventional microstrip lines by increasing the propagation constant as seen in Fig.11. D. Contrary to this in previous section.3. Fig.11. C for SPPs waveguide, it results in stronger confinement of field and therefore, lessening of field overlapping contribution. The reduced coupling and smaller loss in SPPs ultimately make transmission power ratio independent of coupling length. It enables SPPs waveguides more attractive option for designers in dense circuit applications. Experimental results of transmission and coupling ratios in 0.03 - 20GHz range (Fig.15. (D)) also confirmed the accuracy of simulated results. Below the cutoff frequency, both SPPs and MS waveguides show nearly the similar transmission characteristics. On average, 10 dB reduced crosstalk in SPPs is seen which is further reduced by 40dB at 11GHz compared to the microstrip line, therefore proving SPPs as a potential candidate in high-end circuit designs requiring reduced electromagnetic interference.

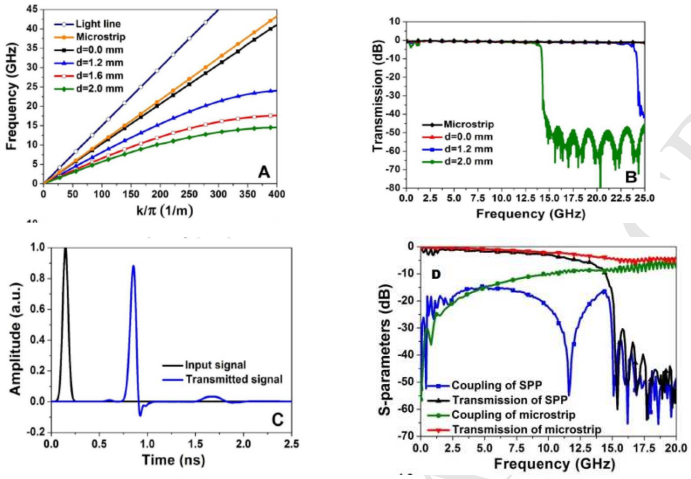

Fig. 15. (i) Dispersion diagrams for varying groove depths. (ii) Simulated transmission Characteristics of different transmission lines. (iii) Simulated time-domain SPP signal with Gaussian pulse input and wide-band of 0-12 GHz. (iv) The measured transmission and coupling coefficients of two closely-packed SPP waveguides and MS lines. [61]

Yang et al. (2015) demonstrated a technique to trap the SPP waves on ultrathin corrugated metallic plates at microwave and terahertz frequencies [108]. Non-uniform corrugations on a very thin metal strip are designed and fabricated based on an ultrathin, flexible dielectric substrate by etching grooves of gradient depth (Fig.16.) to guide the slow SPPs waves and reducing the group velocity steadily. When the frequency is varied, the spoof SPPs are reflected at pre-defined locations. When grooves depths are increased from 4mm to 7mm, dispersion curves move away from the light line thus, lowering the cutoff frequency. It proves stronger confinement of SPPs waves. It has further been demonstrated that with the increase in grooves depth (4.6-6.7mm), the group velocities of spoof SPP waves decrease along the propagation direction on the corrugations of metallic strip. The group velocity can even be decreased to zero at required positions for certain frequencies, through appropriate designing of grooves depths. Electric field distributions plots along the central axis of the strip facilitate to spot the accurate locations of SPPs. Electric field distribution results along the central line of the metallic strip are investigated by numerical simulations and measurements (Fig. 17.), for efficient trapping of SPP waves at desired locations and different frequencies between 9 to 11 GHz. Demonstrated design and method can efficiently be employed in slow wave applications in MW and THz frequencies spectrum.

Fig.16. The photograph of the ultrathin non-uniform corrugated metallic strip [108]

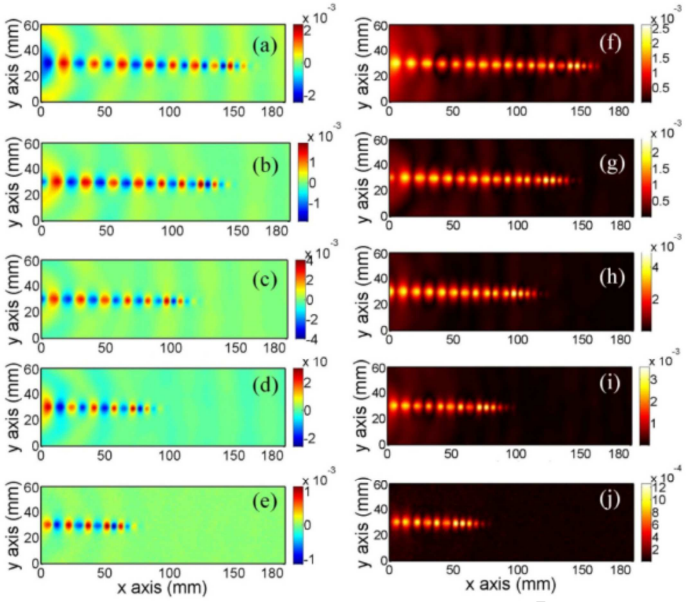

Fig.17. Measured transient-field (a-e) and magnitude distributions (f-j) of electric fields at different frequencies from 9.0 to 11.0 GHz with 0.5GHz increment. [108]

Liu et al. (2015) [51] presented a simple surface plasmon waveguide (SPW) to achieve dual band transmission of spoof SPPs. It has a copper layer on the top having periodic subwavelength holes; Rogers RT6010 is employed as dielectric substrate (Ɛr=10.2, tanδ=0.0023) in the middle while the copper ground layer is added in the bottom of the structure as in Fig. 18. [51].

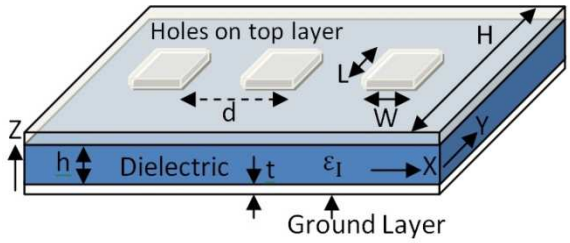

Fig. 18. Sketch of surface plasmonic waveguide having corrugated holes on metal strip separated from a ground layer by a dielectric substrate of thickness h [51].

In practical design, a tapered microstrip line having periodic gradient grooves is realized for effective mode conversion between quasi-transverse EM mode in conventional MS line and spoof SPPs in the plasmonic waveguide. Dispersion curves for fundamental (first mode) and next higher (second mode) mode

are drawn to observe the coupling response for two cases; i.e. with a ground plane and without a ground plane. A strong coupling exists between the corrugated metal strip and the ground layer. Hence, the dispersion curves in the first mode deviate from the light line and lowering the plasma frequency as compared to SPW without a ground layer. Second mode exhibits a negative group velocity band that results in stronger field confinement in proposed grounded SPW as compared to the case without ground at the same frequency. In Fig. 19, dispersion graphs are drawn with variation in hole length L from 0.5mm to 4.5mm for first and second modes of SSPPs, showing results for both cases; with and without a ground layer. Gray shaded area exhibits the expected data in between, with a variation in hole length from minimum to maximum. It is evident that with the increase of hole length, wavevector gradually deviates from the light line, and cutoff frequencies are reduced. Therefore, effective impedance matching is achieved from 50-ohm microstrip line to that of SPW, with the use of gradient holes. Straight and curved hybrid SPWs have been designed (Fig.20.) by adding two transition parts with symmetrical and gradient subwavelength holes to validate the efficiency of the design experimentally and through simulations, both of which agreed very well with each other. For straight SPW, dual transmission bands are observed with first band in 1GHz to 6.5GHz range (S11 < -13dB, S21 > -0.6dB), second band (S11 < -10dB, S21 > -2dB) for 11.5GHz to 13GHz range as seen in Fig. 20.ib. For curved SPW, dual transmission bands are seen in Fig.20. iib. with the first band from 1GHz to 6GHz band (S11 < -10dB, S2 1> -0.8dB) and second band for 12GHz to 13GHz (S11 < -10dB, S21 > -2dB). These verifications declared that the structure is best applicable in low crosstalk transmission applications and smart SSSPs devices in THz and microwave regime.

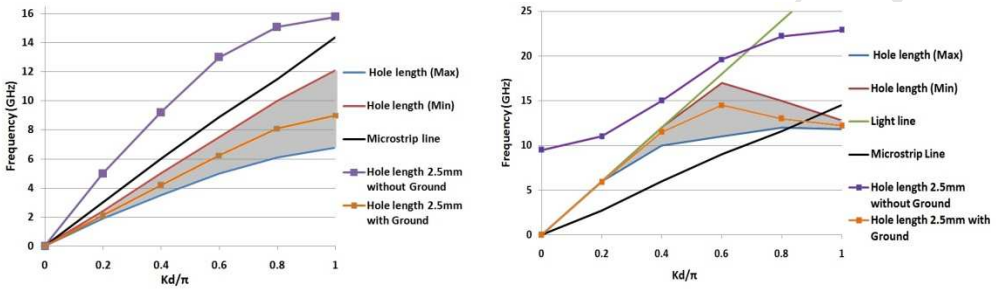

Fig. 19. Dispersion graphs with a variation of hole size from minimum to maximum, for first mode (left) and second modes (right) of SSPPs showing both cases for with and without ground [51] .

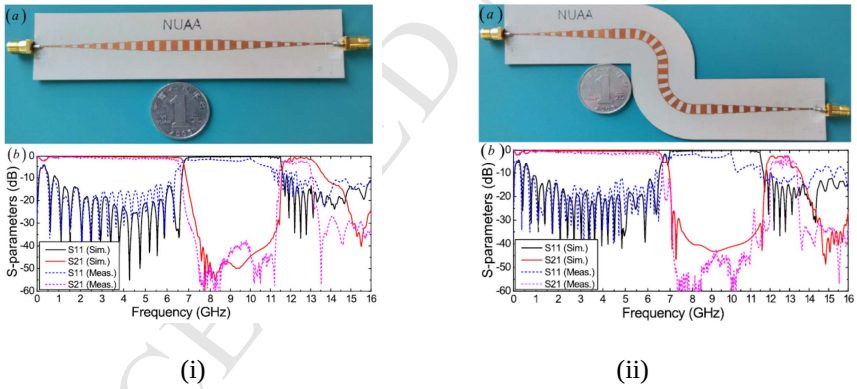

Fig. 20. Photograph of the fabricated SPW with comparison of simulated and measured S-parameters (ia and ib) straight SPW (iia and iib) Curved SPW.[51]

Yin et al. (2015) presented an ultra thin metallic frequency selective plasmonic structure printed on a flexible and thin substrate layer [120]. The structure is based on two metallic strips oppositely oriented and both are corrugated on single side. These are then coupled to another double sided corrugated strip Fig. 21. (i). The structure is fed by traditional coplanar waveguide and extraction of SPPs takes place by designing two transition sections, to smoothly convert between spatial modes in CPW and SPPs modes. Reflection coefficient less than -10dB and transmission loss of 1.5dB have been reported through simulations and measurements in the frequency range of 7 to10 GHz Fig.21. (ii & iii). Proposed spoof SPPs structure can be employed as compact plasmonic pass-band filter with low transmission loss and broader bandwidth and hence, may be applied in multilayer structures for integrated devices and circuits at MW regime.

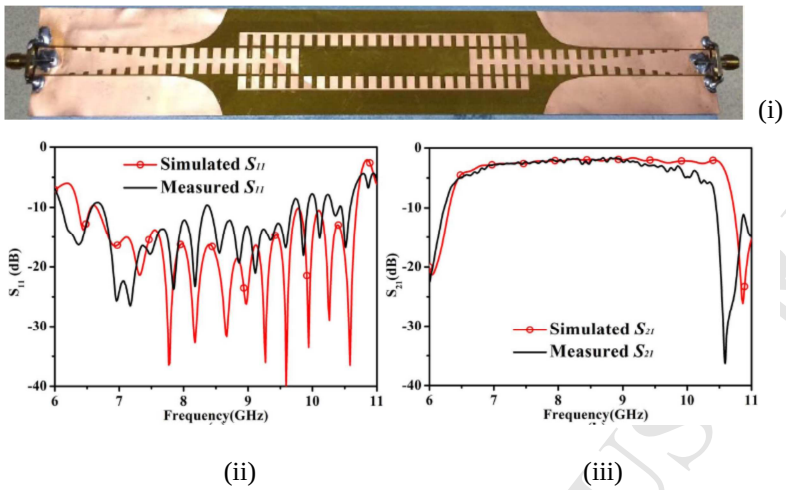

Fig. 21. (i) Photograph of the fabricated SPP structure (ii) and (iii) comparison of simulated and measured S-parameters

Zhang et al. (2016) presented a unique procedure [95] to lessen the microwave transmission line losses by using the feature of designable wavenumber [48], through designing the Spoof SPPs structure at microwave frequencies. An ultrathin, flexible, coplanar surface plasmonic waveguide structure is demonstrated. Gradient, asymmetric periodic corrugations in the metal strip are engineered and for comparison, a similar tapered coplanar microstrip line is also presented with the same geometry (Fig. 22.). Numerical simulation results support that TL losses are reasonably smaller in designed SPPs TL for 2-10 GHz range. Dispersion curves exhibited divergence from the light line with the increase in grooves depths. In a particular frequency range, SPP TLs have smaller wavenumber as compared to MS line and consequently, support mode of propagations with the looser field. With the increase in the value of loss tangent (0.01 to 0.03), transmission properties of SSPPs show a little deviation while for MS line; it is notably deteriorated as seen in Fig. 23 (approximate plots). It is seen that transmission curves intersect at 11.4GHz when both types of TLs are simulated with different values of loss tangent, no matter what the loss tangent of the dielectric substrate is. It is also demonstrated that by keeping the constant value of loss tangent and increasing substrate thickness (0.5mm to 2mm), TLs losses in SPPs become larger while in comparison, TL losses in MS are more stable. The reason is that in MS at low frequency, EM fields are more confined within dielectric substrate. In contrast for SPP TLs, EM field is divided between air and substrate at low frequency. Thus field remains within the dielectric substrate with the increase in its thickness, and therefore, results in the increase of TL losses. Despite the fact, TL loss is comparatively smaller in SPP TL than microstrip case in 2 to 8 GHz frequency band. Further investigations prove that transmission coefficient of SPP TLs is approx 4dB higher than MS line for 3 to 10.5 GHz therefore, confirming a 2.5 times higher transmitted power in SPP transmission line than MS.

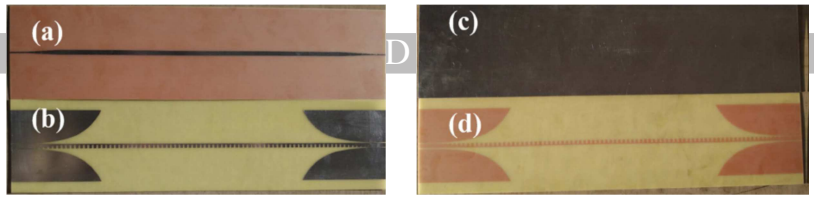

Fig. 22. Photograph of the fabricated structure. Top view of (a) MS TL (b) SSPP TL. Bottom view of (c) MS TL (d) SSPP TL. [95]

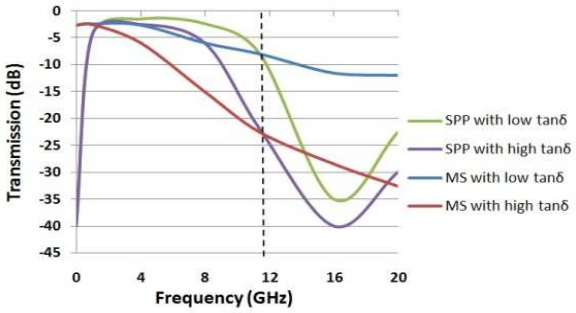

Fig. 23. Transmission spectra of Spoof SPPs and microstrip TLs with variation in loss- tangent. [95]

1. Conclusions

It is evident that plasmonics has sufficiently achieved a maturity level for the designers to implement the phenomenon in practical applications by controlling and confining EM waves on subwavelength scale MW and THz range. In this review article, beside of providing basic concepts of SPPs and its recent applications, a number of fundamental investigations have also been presented to reveal the most exotic properties of surface plasmon polaritons. A major advantage of employing plasmonic metamaterials structures in the realization of SPPs, is the simplicity in design and therefore they are easy to fabricate. The most interesting benefit of SPPs is that the working frequency and EM properties closely depend on the geometric parameters of the structures; giving liberty in their realization at microwave and terahertz frequencies. By designing ultrathin planar and flexible plasmonic structures compact-sized SPP waveguides, devices, circuits, and systems can be produced. The only bottleneck in realizing spoof SPPs devices and circuit lie in the fact that they are required to be bridged to the traditional microwave (MS or CPW) circuitry for smooth and high-efficiency conversion of spatial modes in CPW and SPP modes. It is prominent from thorough researches that the plasmonic structures are proving promising candidate in numerous MW and THz applications. Advances in the subject field up till now are quite extensive. Even more research is likely to be done, and further breakthroughs are anticipated in the near future.

Conflict of Interests

The authors declare that there is no conflict of interests regarding the publication of this paper.

Acknowledgement

This work was funded by the National Natural Science Foundation of China (Grant No.61471035, GrantNo.61603032, and Grant No.61672131), the Fundamental Research Funds for Central Universities

(Grant No.06105031), and the National Key Technologies R&D Program of China(Grant No.2015BAK38B01).

References

[1] X. Qian, X.-H. Peng, D. O. Ansari, Q. Yin-Goen, G. Z. Chen, D. M. Shin, L. Yang, A. N. Young, M. D. Wang, and S. Nie, "In vivo tumor targeting and spectroscopic detection with surface-enhanced Raman nanoparticle tags," Nature biotechnology, vol. 26, pp. 83-90, 2008.

[2] J. Ä. Ì. Homola, S. S. Yee, and G. n. Gauglitz, "Surface plasmon resonance sensors: review," Sensors and Actuators B: Chemical, vol. 54, pp. 3-15, 1999.

[3] P. Mulvaney, "Surface plasmon spectroscopy of nanosized metal particles," Langmuir, vol. 12, pp. 788-800, 1996.

[4] I. Pockrand, J. Swalen, J. Gordon, and M. Philpott, "Surface plasmon spectroscopy of organic monolayer assemblies," Surface Science, vol. 74, pp. 237-244, 1978.

[5] K. A. Willets and R. P. Van Duyne, "Localized surface plasmon resonance spectroscopy and sensing," Annu. Rev. Phys. Chem., vol. 58, pp. 267-297, 2007.

[6] E. Ozbay, "Plasmonics: merging photonics and electronics at nanoscale dimensions," science, vol. 311, pp. 189-193, 2006.

[7] L. Feng, K. A. Tetz, B. Slutsky, V. Lomakin, and Y. Fainman, "Fourier plasmonics: Diffractive focusing of in-plane surface plasmon polariton waves," Applied Physics Letters, vol. 91, p. 081101, 2007.

[8] J. R. Lakowicz, "Plasmonics in biology and plasmon-controlled fluorescence," Plasmonics, vol. 1, pp. 5-33, 2006.

[9] W. L. Barnes, A. Dereux, and T. W. Ebbesen, "Surface plasmon subwavelength optics," Nature, vol. 424, pp. 824-830, 2003.

[10] L. Yin, V. K. Vlasko-Vlasov, J. Pearson, J. M. Hiller, J. Hua, U. Welp, D. E. Brown, and C. W. Kimball, "Subwavelength focusing and guiding of surface plasmons," Nano letters, vol. 5, pp. 1399-1402, 2005.

[11] J. A. Schuller, E. S. Barnard, W. Cai, Y. C. Jun, J. S. White, and M. L. Brongersma, "Plasmonics for extreme light concentration and manipulation," Nature materials, vol. 9, pp. 193-204.

[12] H. A. Atwater and A. Polman, "Plasmonics for improved photovoltaic devices," Nature materials, vol. 9, pp. 205-213.

[13] S. Pillai and M. Green, "Plasmonics for photovoltaic applications," Solar Energy Materials and Solar Cells, vol. 94, pp. 1481-1486.

[14] K. Catchpole and A. Polman, "Design principles for particle plasmon enhanced solar cells," Applied Physics Letters, vol. 93, p. 191113, 2008.

[15] N. Fang, H. Lee, C. Sun, and X. Zhang, "Subâ€“diffraction-limited optical imaging with a silver superlens," science, vol. 308, pp. 534-537, 2005.

[16] I. I. Smolyaninov, J. Elliott, A. V. Zayats, and C. C. Davis, "Far-field optical microscopy with a nanometer-scale resolution based on the in-plane image magnification by surface plasmon polaritons," Physical review letters, vol. 94, p. 057401, 2005.

[17] R. F. Oulton, V. J. Sorger, T. Zentgraf, R.-M. Ma, C. Gladden, L. Dai, G. Bartal, and X. Zhang, "Plasmon lasers at deep subwavelength scale," Nature, vol. 461, pp. 629-632, 2009.

[18] D. E. Chang, A. S. SÃ¸rensen, E. A. Demler, and M. D. Lukin, "A single-photon transistor using nanoscale surface plasmons," Nature Physics, vol. 3, pp. 807-812, 2007.

[19] M. Airola, Y. Liu, and S. Blair, "Second-harmonic generation from an array of sub-wavelength metal apertures," Journal of Optics A: Pure and Applied Optics, vol. 7, p. S118, 2005.

[20] C. R. Yonzon, E. Jeoung, S. Zou, G. C. Schatz, M. Mrksich, and R. P. Van Duyne, "A comparative analysis of localized and propagating surface plasmon resonance sensors: the binding of concanavalin A to a monosaccharide functionalized self-assembled monolayer," Journal of the American Chemical Society, vol. 126, pp. 12669-12676, 2004.

[21] G. Raschke, S. Kowarik, T. Franzl, C. SÃ¶nnichsen, T. Klar, J. Feldmann, A. Nichtl, and K. KÃ¼rzinger, "Biomolecular recognition based on single gold nanoparticle light scattering," Nano letters, vol. 3, pp. 935-938, 2003.

[22] E. Hutter and J. H. Fendler, "Exploitation of localized surface plasmon resonance," Advanced Materials, vol. 16, pp. 1685-1706, 2004.

[23] C. Jung, S. Yee, and K. Kuhn, "Integrated optics waveguide modulator based on surface plasmon resonance," Journal of lightwave technology, vol. 12, pp. 1802-1806, 1994.

[24] H. Hoekstra, P. Lambeck, G. Krijnen, J. Ctyroky, M. De Minicis, C. Sibilia, O. Conradi, S. Helfert, and R. Pregla, "A COST 240 benchmark test for beam propagation methods applied to an electrooptical modulator based on surface plasmons," Journal of lightwave technology, vol. 16, p. 1921, 1998.

[25] T. Nikolajsen, K. Leosson, and S. I. Bozhevolnyi, "Surface plasmon polariton based modulators and switches operating at telecom wavelengths," Applied Physics Letters, vol. 85, pp. 5833-5835, 2004.

[26] A. Krasavin, A. Zayats, K. MacDonald, and N. Zheludev, "High-contrast modulation of light with light by control of surface plasmon polariton wave coupling," arXiv preprint cond-mat/0405448, 2004.

[27] K. Sasaki and T. Nagamura, "Ultrafast wide range all-optical switch using complex refractive-index changes in a composite film of silver and polymer containing photochromic dye," Journal of applied physics, vol. 83, pp. 2894-2900, 1998.

[28] H. Bethe, "Theory of diffraction by small holes," Physical Review, vol. 66, p. 163, 1944.

[29] R. Ritchie, "Plasma losses by fast electrons in thin films," Physical Review, vol. 106, p. 874, 1957.

[30] C. Powell and J. Swan, "Origin of the characteristic electron energy losses in aluminum," Physical Review, vol. 115, p. 869, 1959.

[31] H. Raether, Surface plasmons on smooth surfaces: Springer, 1988.

[32] T. W. Ebbesen, H. J. Lezec, H. Ghaemi, T. Thio, and P. Wolff, "Extraordinary optical transmission through sub-wavelength hole arrays," Nature, vol. 391, pp. 667-669, 1998.
[33] C. Genet and T. Ebbesen, "Light in tiny holes," Nature, vol. 445, pp. 39-46, 2007.
[34] R. Gordon, A. G. Brolo, D. Sinton, and K. L. Kavanagh, "Resonant optical transmission through holeâ€ arrays in metal films: physics and applications," Laser & Photonics Reviews, vol. 4, pp. 311-335.
[35] F. J. Garcia-Vidal, L. Martin-Moreno, T. Ebbesen, and L. Kuipers, "Light passing through subwavelength apertures," Reviews of Modern Physics, vol. 82, p. 729.
[36] S. G. Rodrigo, F. de LeÃ³n-PÃ©rez, and L. MartÃ-n-Moreno, "Extraordinary optical transmission: fundamentals and applications," Proceedings of the IEEE, vol. 104, pp. 2288-2306.
[37] S. G. Rodrigo, L. MartÃ-n-Moreno, A. Y. Nikitin, A. Kats, I. Spevak, and F. Garcia-Vidal, "Extraordinary optical transmission through hole arrays in optically thin metal films," Optics letters, vol. 34, pp. 4-6, 2009.
[38] L. Martin-Moreno, F. Garcia-Vidal, H. Lezec, K. Pellerin, T. Thio, J. Pendry, and T. Ebbesen, "Theory of extraordinary optical transmission through subwavelength hole arrays," Physical review letters, vol. 86, p. 1114, 2001.
[39] T. Thio, K. Pellerin, R. Linke, H. Lezec, and T. Ebbesen, "Enhanced light transmission through a single subwavelength aperture," Optics letters, vol. 26, pp. 1972-1974, 2001.
[40] W. L. Barnes, W. A. Murray, J. Dintinger, E. Devaux, and T. Ebbesen, "Surface plasmon polaritons and their role in the enhanced transmission of light through periodic arrays of subwavelength holes in a metal film," Physical review letters, vol. 92, p. 107401, 2004.
[41] J. Bravo-Abad, F. GarcÃ-a-Vidal, and L. MartÃ-n-Moreno, "Resonant transmission of light through finite chains of subwavelength holes in a metallic film," Physical review letters, vol. 93, p. 227401, 2004.
[42] A. P. Hibbins, J. R. Sambles, C. R. Lawrence, and J. R. Brown, "Squeezing millimeter waves into microns," Physical review letters, vol. 92, p. 143904, 2004.
[43] C.-C. Chen, "Transmission through a conducting screen perforated periodically with apertures," IEEE Transactions on Microwave Theory and Techniques, vol. 18, pp. 627-632, 1970.
[44] G. Goubau, "Surface waves and their application to transmission lines," Journal of applied physics, vol. 21, pp. 1119-1128, 1950.
[45] J. R. Wait, "The ancient and modern history of EM ground-wave propagation," IEEE Antennas and Propagation Magazine, vol. 40, pp. 7-24, 1998.
[46] M. WÃ¥chter, M. Nagel, and H. Kurz, "Frequency-dependent characterization of THz Sommerfeld wave propagation on single-wires," Optics Express, vol. 13, pp. 10815-10822, 2005.
[47] S. A. Maier, Plasmonics: fundamentals and applications: Springer Science & Business Media, 2007.
[48] J. Pendry, L. Martin-Moreno, and F. Garcia-Vidal, "Mimicking surface plasmons with structured surfaces," science, vol. 305, pp. 847-848, 2004.
[49] A. P. Hibbins, B. R. Evans, and J. R. Sambles, "Experimental verification of designer surface plasmons," science, vol. 308, pp. 670-672, 2005.
[50] F. Garcia-Vidal, L. Martin-Moreno, and J. Pendry, "Surfaces with holes in them: new plasmonic metamaterials," Journal of Optics A: Pure and Applied Optics, vol. 7, p. S97, 2005.
[51] L. Liu, Z. Li, B. Xu, P. Ning, C. Chen, J. Xu, X. Chen, and C. Gu, "Dual-band trapping of spoof surface plasmon polaritons and negative group velocity realization through microstrip line with gradient holes," Applied Physics Letters, vol. 107, p. 201602.
[52] S. Berry, T. Campbell, A. P. Hibbins, and J. R. Sambles, "Surface wave resonances supported on a square array of square metallic pillars," Applied Physics Letters, vol. 100, p. 101107.
[53] Q. Gan, Y. Gao, K. Wagner, D. Vezenov, Y. J. Ding, and F. J. Bartoli, "Experimental verification of the rainbow trapping effect in adiabatic plasmonic gratings," Proceedings of the National Academy of Sciences, vol. 108, pp. 5169-5173.
[54] C. R. Williams, S. R. Andrews, S. Maier, A. FernÃ¡ndez-DomÃ-nguez, L. MartÃ-n-Moreno, and F. GarcÃ-a-Vidal, "Highly confined guiding of terahertz surface plasmon polaritons on structured metal surfaces," Nature Photonics, vol. 2, pp. 175-179, 2008.
[55] S. A. Maier, S. R. Andrews, L. Martin-Moreno, and F. Garcia-Vidal, "Terahertz surface plasmon-polariton propagation and focusing on periodically corrugated metal wires," Physical review letters, vol. 97, p. 176805, 2006.
[56] J. G. m. Rivas, "Terahertz: The art of confinement," Nature Photonics, vol. 2, pp. 137-138, 2008.
[57] P. Nagpal, N. C. Lindquist, S.-H. Oh, and D. J. Norris, "Ultrasmooth patterned metals for plasmonics and metamaterials," science, vol. 325, pp. 594-597, 2009.
[58] Y. Jin Zhou, Q. Jiang, and T. Jun Cui, "Bidirectional bending splitter of designer surface plasmons," Applied Physics Letters, vol. 99, p. 111904.
[59] Q. Gan, Z. Fu, Y. J. Ding, and F. J. Bartoli, "Ultrawide-bandwidth slow-light system based on THz plasmonic graded metallic grating structures," Physical review letters, vol. 100, p. 256803, 2008.
[60] D. MartÃ-n-Cano, M. Nesterov, A. Fernandez-Dominguez, F. Garcia-Vidal, L. Martin-Moreno, and E. Moreno, "Plasmons for subwavelength terahertz circuitry," Optics Express, vol. 18, pp. 754-764.
[61] H. C. Zhang, T. J. Cui, Q. Zhang, Y. Fan, and X. Fu, "Breaking the challenge of signal integrity using time-domain spoof surface plasmon polaritons," ACS photonics, vol. 2, pp. 1333-1340.
[62] X. Shen and T. J. Cui, "Planar plasmonic metamaterial on a thin film with nearly zero thickness," Applied Physics Letters, vol. 102, p. 211909.
[63] X. Gao, L. Zhou, Z. Liao, H. F. Ma, and T. J. Cui, "An ultra-wideband surface plasmonic filter in microwave frequency," Applied Physics Letters, vol. 104, p. 191603.
[64] X. Gao and T. J. Cui, "Spoof surface plasmon polaritons supported by ultrathin corrugated metal strip and their applications," Nanotechnology Reviews, vol. 4, pp. 239-258.

[65] H. F. Ma, X. Shen, Q. Cheng, W. X. Jiang, and T. J. Cui, "Broadband and highâ€ efficiency conversion from guided waves to spoof surface plasmon polaritons," Laser & Photonics Reviews, vol. 8, pp. 146-151.
[66] X. Shen, T. J. Cui, D. Martin-Cano, and F. J. Garcia-Vidal, "Conformal surface plasmons propagating on ultrathin and flexible films," Proceedings of the National Academy of Sciences, vol. 110, pp. 40-45.
[67] H. C. Zhang, S. Liu, X. Shen, L. H. Chen, L. Li, and T. J. Cui, "Broadband amplification of spoof surface plasmon polaritons at microwave frequencies," Laser & Photonics Reviews, vol. 9, pp. 83-90.
[68] X. Shen and T. J. Cui, "Ultrathin plasmonic metamaterial for spoof localized surface plasmons," Laser & Photonics Reviews, vol. 8, pp. 137-145.
[69] P. A. Huidobro, X. Shen, J. Cuerda, E. Moreno, L. Martin-Moreno, F. Garcia-Vidal, T. J. Cui, and J. Pendry, "Magnetic localized surface plasmons," Physical Review X, vol. 4, p. 021003.
[70] J. O'Hara, R. Averitt, and A. Taylor, "Terahertz surface plasmon polariton coupling on metallic gratings," Optics Express, vol. 12, pp. 6397-6402, 2004.
[71] J. F. Oâ€™Hara, R. D. Averitt, and A. J. Taylor, "Prism coupling to terahertz surface plasmon polaritons," Optics Express, vol. 13, pp. 6117-6126, 2005.
[72] J. Saxler, J. G. m. Rivas, C. Janke, H. Pellemans, P. H. Bolivar, and H. Kurz, "Time-domain measurements of surface plasmon polaritons in the terahertz frequency range," Physical Review B, vol. 69, p. 155427, 2004.
[73] V. M. Shalaev and S. Kawata, Nanophotonics with surface plasmons: Elsevier, 2006.
[74] D. Qu, D. Grischkowsky, and W. Zhang, "Terahertz transmission properties of thin, subwavelength metallic hole arrays," Optics letters, vol. 29, pp. 896-898, 2004.
[75] A. K. Azad, Y. Zhao, and W. Zhang, "Transmission properties of terahertz pulses through an ultrathin subwavelength silicon hole array," Applied Physics Letters, vol. 86, p. 141102, 2005.
[76] H. Cao and A. Nahata, "Resonantly enhanced transmission of terahertz radiation through a periodic array of subwavelength apertures," Optics Express, vol. 12, pp. 1004-1010, 2004.
[77] J. G. m. Rivas, C. Schotsch, P. H. Bolivar, and H. Kurz, "Enhanced transmission of THz radiation through subwavelength holes," Physical Review B, vol. 68, p. 201306, 2003.
[78] C. Janke, J. G. m. Rivas, C. Schotsch, L. Beckmann, P. H. Bolivar, and H. Kurz, "Optimization of enhanced terahertz transmission through arrays of subwavelength apertures," Physical Review B, vol. 69, p. 205314, 2004.
[79] E. Hendry, M. J. Lockyear, J. G. m. Rivas, L. Kuipers, and M. Bonn, "Ultrafast optical switching of the THz transmission through metallic subwavelength hole arrays," Physical Review B, vol. 75, p. 235305, 2007.
[80] A. K. Azad, H.-T. Chen, S. R. Kasarla, A. J. Taylor, Z. Tian, X. Lu, W. Zhang, H. Lu, A. C. Gossard, and J. F. Oâ€™Hara, "Ultrafast optical control of terahertz surface plasmons in subwavelength hole arrays at room temperature," Applied Physics Letters, vol. 95, p. 011105, 2009.
[81] Z. Tian, A. K. Azad, X. Lu, J. Gu, J. Han, Q. Xing, A. J. Taylor, J. F. Oâ€™Hara, and W. Zhang, "Large dynamic resonance transition between surface plasmon and localized surface plasmon modes," Optics Express, vol. 18, pp. 12482-12488.
[82] X. Shou, A. Agrawal, and A. Nahata, "Role of metal film thickness on the enhanced transmission properties of a periodic array of subwavelength apertures," Optics Express, vol. 13, pp. 9834-9840, 2005.
[83] A. K. Azad, Y. Zhao, W. Zhang, and M. He, "Effect of dielectric properties of metals on terahertz transmission in subwavelength hole arrays," Optics letters, vol. 31, pp. 2637-2639, 2006.
[84] B. Ferguson and X.-C. Zhang, "Materials for terahertz science and technology," Nature materials, vol. 1, pp. 26-33, 2002.
[85] R. Huber, F. Tauser, A. Brodschelm, M. Bichler, G. Abstreiter, and A. Leitenstorfer, "How many-particle interactions develop after ultrafast excitation of an electronâ€“hole plasma," Nature, vol. 414, pp. 286-289, 2001.
[86] M. Nagel, P. H. Bolivar, M. Brucherseifer, H. Kurz, A. Bosserhoff, and R. BÃ¼ttner, "Integrated THz technology for label-free genetic diagnostics," Applied Physics Letters, vol. 80, pp. 154-156, 2002.
[87] D. Grischkowsky, S. r. Keiding, M. Van Exter, and C. Fattinger, "Far-infrared time-domain spectroscopy with terahertz beams of dielectrics and semiconductors," JOSA B, vol. 7, pp. 2006-2015, 1990.
[88] W. Zhang, A. K. Azad, and D. Grischkowsky, "Terahertz studies of carrier dynamics and dielectric response of n-type, freestanding epitaxial GaN," Applied Physics Letters, vol. 82, pp. 2841-2843, 2003.
[89] D. M. Mittleman, R. H. Jacobsen, and M. C. Nuss, "T-ray imaging," IEEE Journal of selected topics in quantum electronics, vol. 2, pp. 679-692, 1996.
[90] M. C. Beard, G. M. Turner, and C. A. Schmuttenmaer, "Subpicosecond carrier dynamics in low-temperature grown GaAs as measured by time-resolved terahertz spectroscopy," Journal of applied physics, vol. 90, pp. 5915-5923, 2001.
[91] J. Federici and L. Moeller, "Review of terahertz and subterahertz wireless communications," Journal of applied physics, vol. 107, p. 111101.
[92] Y. Shen, T. Lo, P. Taday, B. Cole, W. Tribe, and M. Kemp, "Detection and identification of explosives using terahertz pulsed spectroscopic imaging," Applied Physics Letters, vol. 86, p. 241116, 2005.
[93] J. F. Oâ€™Hara, W. Withayachumnankul, and I. Al-Naib, "A review on thin-film sensing with terahertz waves," Journal of Infrared, Millimeter, and Terahertz Waves, vol. 33, pp. 245-291.
[94] M. Nagel, M. FÃ¶rst, and H. Kurz, "THz biosensing devices: fundamentals and technology," Journal of Physics: Condensed Matter, vol. 18, p. S601, 2006.
[95] H. C. Zhang, Q. Zhang, J. F. Liu, W. Tang, Y. Fan, and T. J. Cui, "Smaller-loss planar SPP transmission line than conventional microstrip in microwave frequencies," Scientific reports, vol. 6.
[96] J. J. Wu, D. J. Hou, K. Liu, L. Shen, C. A. Tsai, C. J. Wu, D. Tsai, and T.-J. Yang, "Differential microstrip lines with reduced crosstalk and common mode effect based on spoof surface plasmon polaritons," Optics Express, vol. 22, pp. 26777-26787.
[97] R. Ulrich, "Far-infrared properties of metallic mesh and its complementary structure," Infrared Physics, vol. 7, pp. 37-55, 1967.

[98] C. M. Rhoads, E. K. Damon, and B. A. Munk, "Mid-infrared filters using conducting elements," Applied optics, vol. 21, pp. 2814-2816, 1982.
[99] C. Winnewisser, F. Lewen, J. Weinzierl, and H. Helm, "Transmission features of frequency-selective components in the far infrared determined by terahertz time-domain spectroscopy," Applied optics, vol. 38, pp. 3961-3967, 1999.
[100] L. Liu, Z. Li, B. Xu, P. Ning, C. Chen, and C. Gu, "An ultra-wideband low-pass plasmonic filter based on spoof surface plasmon polaritons," in 2015 Asia-Pacific Microwave Conference (APMC), pp. 1-3.
[101] B. C. Pan, Z. Liao, J. Zhao, and T. J. Cui, "Controlling rejections of spoof surface plasmon polaritons using metamaterial particles," Optics Express, vol. 22, pp. 13940-13950.
[102] L. Liu, Z. Li, C. Gu, P. Ning, B. Xu, Z. Niu, and Y. Zhao, "Multi-channel composite spoof surface plasmon polaritons propagating along periodically corrugated metallic thin films," Journal of applied physics, vol. 116, p. 013501.
[103] Z. Liao, J. Zhao, B. C. Pan, X. P. Shen, and T. J. Cui, "Broadband transition between microstrip line and conformal surface plasmon waveguide," Journal of Physics D: Applied Physics, vol. 47, p. 315103.
[104] X. Gao, L. Zhou, and T. J. Cui, "Odd-mode surface plasmon polaritons supported by complementary plasmonic metamaterial," Scientific reports, vol. 5, p. 9250.
[105] W. Zhang, G. Zhu, L. Sun, and F. Lin, "Trapping of surface plasmon wave through gradient corrugated strip with underlayer ground and manipulating its propagation," Applied Physics Letters, vol. 106, p. 021104.
[106] F. Pavanello, F. d. r. Garet, M.-B. Kuppam, E. Peytavit, M. Vanwolleghem, F. o. Vaurette, J.-L. Coutaz, and J.-F. o. Lampin, "Broadband ultra-low-loss mesh filters on flexible cyclic olefin copolymer films for terahertz applications," Applied Physics Letters, vol. 102, p. 111114.
[107] T. F. Krauss, "Why do we need slow light?," Nature Photonics, vol. 2, pp. 448-450, 2008.
[108] Y. Yang, X. Shen, P. Zhao, H. C. Zhang, and T. J. Cui, "Trapping surface plasmon polaritons on ultrathin corrugated metallic strips in microwave frequencies," Optics Express, vol. 23, pp. 7031-7037.
[109] A. V. Zayats, I. I. Smolyaninov, and A. A. Maradudin, "Nano-optics of surface plasmon polaritons," Physics reports, vol. 408, pp. 131-314, 2005.
[110] S. A. Ramakrishna, "Physics of negative refractive index materials," Reports on Progress in Physics, vol. 68, p. 449, 2005.
[111] R. E. Collin, "Field theory of guided waves," 1960.
[112] M. Van Exter and D. Grischkowsky, "Optical and electronic properties of doped silicon from 0.1 to 2 THz," Applied Physics Letters, vol. 56, pp. 1694-1696, 1990.
[113] N. Katzenellenbogen and D. Grischkowsky, "Electrical characterization to 4 THz of Nâ€ and Pâ€ type GaAs using THz timeâ€ domain spectroscopy," Applied Physics Letters, vol. 61, pp. 840-842, 1992.
[114] D. B. Beam, "Characterization of optically dense, doped semiconductors by reflection THz time domain spectroscopy," Applied Physics Letters, vol. 72, 1998.
[115] A. K. Azad, J. F. O'Hara, R. Singh, H.-T. Chen, and A. J. Taylor, "A review of terahertz plasmonics in subwavelength holes on conducting films," IEEE Journal of Selected Topics in Quantum Electronics, vol. 19, pp. 8400416-8400416.
[116] J. G. m. Rivas, P. H. Bolivar, and H. Kurz, "Thermal switching of the enhanced transmission of terahertz radiation through subwavelength apertures," Optics letters, vol. 29, pp. 1680-1682, 2004.
[117] C. Janke, J. G. m. Rivas, P. H. Bolivar, and H. Kurz, "All-optical switching of the transmission of electromagnetic radiation through subwavelength apertures," Optics letters, vol. 30, pp. 2357-2359, 2005.
[118] W. Zhang, A. K. Azad, J. Han, J. Xu, J. Chen, and X.-C. Zhang, "Direct observation of a transition of a surface plasmon resonance from a photonic crystal effect," Physical review letters, vol. 98, p. 183901, 2007.
[119] S. Enoch and N. Bonod, Plasmonics: from basics to advanced topics vol. 167: Springer.
[120] J. Y. Yin, J. Ren, H. C. Zhang, B. C. Pan, and T. J. Cui, "Broadband frequency-selective spoof surface plasmon polaritons on ultrathin metallic structure," Scientific reports, vol. 5, p. 8165.